Variation of Uncertainty of Drainage Density in Flood Hazard Mapping Assessment with Coupled 1D-2D Hydrodynamics Model

Song-Yue Yang (acton0910@gmail.com)
Feng Chia University https://orcid.org/0000-0002-8428-0892
Che-Hao Chang
National Taipei University of Technology
Chih-Tsung Hsu
National Applied Research Laboratories National Center for High-Performance Computing
Shiang-Jen Wu
National United University

Research Article

Keywords: uncertainty, drainage density, flood hazard mapping, 1D-2D hydrodynamics model

Posted Date: June 7th, 2021

DOI: https://doi.org/10.21203/rs.3.rs-203686/v1

Version of Record: A version of this preprint was published at Natural Hazards on January 19th, 2022.
See the published version at https://doi.org/10.1007/s11069-021-05138-1.

Variation of Uncertainty of Drainage Density in Flood Hazard Mapping Assessment with Coupled 1D-2D Hydrodynamics Model

Song-Yue Yang[1], Che-Hao Chang[2]*, Chih-Tsung Hsu[3], Shiang-Jen Wu[4]

Song-Yue Yang (acton0910@gmail.com); ORDIC: 0000-0002-8428-0892

Che-Hao Chang (fencerc@gmail.com); ORDIC: 0000-0002-0965-5471

Chih-Tsung Hsu (hsu.nelson31@gmail.com)

Shiang-Jen Wu (sjwu@nuu.edu.tw)

[1] Department of Urban Planning and Spatial Information, Feng Chia University, No.100, Wenhwa Rd., Seatwen Dist., Taichung 40724, Taiwan

[2] Department of Civil Engineering, National Taipei University of Technology, No. 1, Sec. 3, Zhongxiao E. Rd., Taipei 10608, Taiwan

[3] National Center for High-Performance Computing, National Applied Research Laboratories, No. 7, R&D 6th Rd., Hsinchu Science Park, Hsinchu 30076, Taiwan

[4] Department of Civil and Disaster Prevention Engineering, National United University, No. 2, Lienda, Miaoli 360001, Taiwan,

Correspondence to: Che-Hao Chang (fencerc@gmail.com)

Acknowledgements

This research project is funded by the Ministry of Science and Technology, Taiwan (grant numbers MOST 109-2625-M-035-007-MY3). The authors thank Mr. George Chih-Yu Chen for his assistance in the English editing, and Mr. Cheng-Hsuan Wu for his assistance in the experiments.

Declarations

Funding

This research project is funded by the Ministry of Science and Technology, Taiwan (grant numbers MOST 109-2625-M-035-007-MY3)

Conflicts of interest/Competing interests

The authors declare that they have no competing interests.

Availability of data and material

The data that support the findings of this study are available from the corresponding author, Che-Hao Chang, upon reasonable request.

Code availability (software application or custom code)

SOBEK model (version 2.13) developed by Deltares were used in this study.

Authors' contributions

Song-Yue Yang wrote the paper; Che-Hao Chang performed the experiments; Chih-Tsung Hsu built the models; Shiang-Jen Wu reviewed the paper.

Abstract Coupled 1D-2D hydrodynamic models are widely utilized in flood hazard mapping. Researchers have explored several uncertainties in flood hazard mapping, but have not addressed the uncertainty of drainage density. Drainage density is equal to total length of the drainage divided by the catchment area. The model sets denser the tributary drainages for higher drainage density values. This study uses a designed case and a real case, Yanshuixi Drainage in Tainan, Taiwan, to assess the uncertainty of drainage density in flood hazard mapping. Analytical results indicate that under the same return period rainfall, reduction in tributary drainages in a model (indicating a lower drainage density) results in an underestimate of the flooded area in tributary drainages. This underestimate causes higher peak discharges and total volume of discharges in the drainages, leading to flooding in certain downstream reaches, thereby overestimating the flooded area. The uncertainty of drainage density decreases with increased rainfall. We suggest that modeling flood hazard mapping with low return period rainfalls requires tributary drainages. For extreme rainfall events, a lower drainage density could be selected, but the drainage density of local key areas should be raised.

Keywords uncertainty · drainage density · flood hazard mapping · 1D-2D hydrodynamics model

1 Introduction

In coupled one-dimensional and two-dimensional hydrodynamics models (1D-2D model), the channel flows are simulated in a 1D model, and the floodplain flows are simultaneously simulated in 2D. Two-dimensional hydrodynamics schemes include simple-volume conservative storage-filling algorithms, diffusive wave scheme and fully dynamic shallow water modelling. Since 1D-2D models have high accuracy and short calculation time, it is widely used in Meso (regional) scale and Micro (local) scale flood hazard assessment (Apel *et al*. 2009; de Moel *et al*. 2015; Werner 2004; Werner *et al*. 2005) . Wilson *et al*. (2007) adopted 1D-2D model LISFLOOD-FP and topographic data from the Shuttle Radar Topography Mission to derive the inundation of Amazonian seasonally flooded wetlands. Price and Vojinovic (2008) proposed the use of the concept of digital city to manage urban flood disasters, based on the tropical island of St Maarten, one of five land area of the Netherlands Antilles. The flood hazard maps were simulated with the flooding model MIKE 11 package developed by DHI Water and Environment. Timbadiya *et al*. (2015) used a 1D-2D model (MIKE 11 and MIKE 21) to forecast the water level of lower Tapi River in India. The flood hazard maps in Tainan, Taiwan were simulated using the 1D-2D model SOBEK for flood risk management (Doong et al. 2016). Wu *et al*. (2017) applied a 1D-2D model, coupling the SWMM and LISFLOOD-FP models, to predict the future flooding scenarios in Dongguan, China. Yang *et al.* (2018a; 2018b) used the SOBEK model to evaluate the flood risk transfer effects due to land development in lowlands.

Several sources of uncertainties in 1D-2D models have been widely studied, analyzed and summarized. The main sources of uncertainties for the models include model selection and parameter settings, as well as hydrological and geological data of the models (Bales and Wagner 2009; de Moel *et al*. 2015; Merwade *et al*. 2008; Teng *et al*. 2017). Werner (2004) compared 1D (SOBEK-RIVER), 2D (DELFIT-FLS) and 1D-2D (SOBEK-OVERLAND FLOW) models to predict flood stages of the River Saar in Germany. The research results demonstrated 1D and 1D-2D models generated more reliable simulation results than 2D model. Werner *et al*. (2005) compared SOBEK 1D model and coupled SOBEK 1D-2D model to predict floodplain inundation in the towns of Usti and Orlici in Czech Republic. Their research results show that the simulation results of 1D model and 1D-2D model in the flooded area were similar. However, the 1D-2D model showed better performance in comparison of distributed water level observations. Apel *et al*. (2009) compared linear interpolation methodology, 1D-2D model (LISFLOOD-FP) and 2D models for the risk analysis in the municipality of Eilenburg in Saxony, Germany. The simulation results of the 1D-2D and 2D models were highly consistent with the observed flooding extents and depths. However, the long calculation time required by the 2D model was a major obstacle in the calibration process. Dimitriadis *et al*. (2016) employed a Monte-Carlo approach to analyze the uncertainty of input discharge, longitudinal and lateral gradients, roughness coefficient and the grid size in three 1D and quasi-2D models (HEC-RAS, LISFLOOD-FP, and FLO-2d). Their research result revealed that the

channel and floodplain friction, and inflow discharge were the main uncertainties in flood propagation.

Another major source of model uncertainty is model input, including both hydrological and geological data. Many researchers have examined the design rainfall, inflow hydrograph, lateral discharge, channel and floodplain geometry. Wu *et al*. (2010) developed a risk analysis model, combined with multivariate Monte Carlo simulation and Advance First-Order Second-Moment method. The model was applied to assess the risk of underestimating flood peak flows due to the uncertainties in rainfall information (rainfall depth, duration and storm pattern), and the uncertainties in the parameters of the rainfall-runoff model (Sacramento Soil Moisture Accounting model, SAC-SMA). Wu *et al*. (2011) presented a risk analysis model to measure the risk of damage to the flood protection structure of the Keelung River due to uncertainties in hydrology and hydraulic analysis, including hydrological, hydraulic, and geomorphologic uncertainty. Their analytical results revealed that hydrological uncertainty had a greater impact than hydraulic and geomorphological uncertainty. Wong *et al*. (2015) used a 1D-2D model (LISFLOOD-FP) to study the effect of river channel cross-section and longitudinal-section geometry on flood dynamics. Their results indicated that uncertainty on channel longitudinal-section variability only affected the local flood dynamics, but did not significantly affect the friction sensitivity or inundation mapping. These effects were negligible, as they were less important than other uncertainties, such as boundary conditions.

The grid resolution and the post-processing quality significantly influence the flood simulation results. Adeogun *et al*. (2015) proposed a 1D-2D model, coupling 1D sewer model (SWMM) and 2D inundation model, and analyzed the sensitivity of the mesh resolution and roughness. The research results revealed that a higher-resolution mesh enhanced the flooding simulation results, but lengthened the calculation time. Noh *et al*. (2018) developed a hybrid parallel code (H12) of the 1D-2D model to accelerate the calculation speed of the flood simulations with a hyper-resolution grid. Their research results showed that the hyper-resolution grid modeling accurately described the flooding situation in urban areas, while the coarser resolution grid modeling led to local isolation and distortion of the flooded area, due to the lack of topographical details. Meesuk *et al*. (2015) presented Multidimensional Fusion of Views-Digital Terrain Model (MFV-DTM) to integrate ground-view Structure from Motion (SfM) observations with top-view LiDAR data. A 1D-2D model was applied to simulate an extreme urban flood event that occurred on June 10, 2003 in Kuala Lumpur, Malaysia. The research results demonstrated that MFV-DTM modeling could represent a true flood situation better than the standard LiDAR-DTM modeling and Filtered LiDAR-DTM modeling.

For flood hazard mapping, in addition to DEM, another important data input in the model is the cross-section and longitudinal-section of the drainages. A river drainage system is quite complex, as in addition to the mainstream of river, it also includes river tributaries, regional drainages, farmland drainages and storm sewers. As far as the authors know, no research has previously been undertaken on the effect of the detailed degree of drainage data in the model on the flood simulation results. The drainage density is equal to total length of the discharges divided by catchment area.

This study set denser the tributary drainages in a model with higher drainage density. Two experiments, simulated by 1D-2D model SOBEK, were executed to explore the uncertainty of drainage density in flood hazard mapping.

2 Materials and Methods

2.1 SOBEK model simulation

The hydrological and hydraulic model was developed using the SOBEK model (version 2.13) developed by Deltares in the Netherlands. The SOBEK model has several modules, including Rainfall-Runoff, 1D FLOW-Rural and Overland Flow-2D (Deltares 2017). In this study, the flooding simulation process consisted of two phases. The first process was the hydrological phase. At this stage, the Rainfall-Runoff module was run to convert rainfall into runoff, and then the discharge of sub-catchment was calculated. The second phase was the hydraulic phase. After the runoff was introduced into the channel, the 1D-2D module was run to perform the calculation with complete Saint Venant equations. When the discharge exceeds the flood capacity of the channel, the water overflows the channel, and then the dynamic flow on the surface was simulated through 2D module. This study employed the US Soil Conservation Service Curve Number method to compute abstractions. In the method, the parameters of the flow path and the slope in the catchment were estimated from DEM, and the parameter of Curve Number was estimated from land use. In the rainfall-runoff model, the US Soil Conservation Service's dimensionless unit hydrograph was utilized to convert rainfall into discharge of the sub-catchment.

2.2 Experiment I

Five different models were designed (as shown in the Table 1). Model 2-yr included Drainages 2-yr, 5-yr, 10-yr, 50-yr, and 100-yr. Model 5-yr included Drainages 5-yr, 10-yr, 50-yr, and 100-yr, and so on (as shown in Fig. 1). A two-yr return period flood could be drained by Drainage 2-yr. A five-yr return period flood could be drained by Drainage 5-yr, and so on. Each model was simulated with 2-yr, 5-yr, 10-yr, 50-yr, and 100-yr return period rainfalls. In each scenario, the flooded area, as well as the peak discharge (Q_A) and the total volume of discharge at Point A (V_A) were calculated and compared.

2.3 Experiment II

2.3.1 study area

This study used the catchment of Yanshuixi Drainage in Tainan, Taiwan as a case study. The Taiwan Strait, Zengwun River and Yanshuei River are situated in the west, north and south of the catchment, respectively. The catchment area is 108.454 km^2, and the terrain is inclined from northeast to southwest. The elevation of the catchment area is between Elevation Level (E.L.) −0.2 m and 9.5 m. The drainage length is 19.20 km, and the average slope is about 1/7,000. The river export is about 315 m wide, and most of the river bank is concrete revetment (see Fig. 2). The

land usages in the catchment of Yanshuixi Drainage are agriculture (42.4 %), forest (1.8 %), traffic (9.9 %), water (5.9 %), build-up (19.3 %), public (2.0 %), recreation (3.0 %), mining (0.1 %) and other (15.6 %). Due to the flat and low terrain, the drainage outlets are affected by the tidal level, and typhoons and heavy rains often cause floods downstream.

2.3.2 Drainage density

In this study, drainage density (D_d) is the total length of all the drainages in a watershed divided by the total area of the watershed.

$$D_d = \frac{L}{A} \tag{1}$$

where:

L: total length of all the drainages in a watershed (km)

A: total area of the watershed (km^2)

Two types of drainages, regional drainage and farmland drainage, were set in models. The total length of regional drainages in Model I was 75.370 km. In Model II, in addition to regional drainages, 50.143 km of farmland drainages was added. Table 2 lists the channel densities of Model I and II, which are 0.695 km^{-1}, and 1.157 km^{-1}, respectively.

This study included regional drainages, and farmland drainages and related hydraulic structures, such as gates, pumping stations, detention basins and bridges, which were all set up in SOBEK. The DEM with an elevation accuracy of 10 ~ 20 cm was evaluated from the Airborne LiDAR point cloud by Ministry of Interior. The grid resolution was set to 20 m. Observed rainfall data from the Quantitative Precipitation Estimation and Segregation Using Multiple Sensor (QPESUMS) were based on 6 Dopper radars of the Central Weather Bureau. The interval of the weather information was 10 minutes, and the grid resolution was 1.3 km (Chiou *et al.* 2005; Wang *et al.* 2016). The boundary condition of the model was based on the tide level of the Sicao tide station. The study area includes three water level stations, labeled in Fig. 2 as Stations 1, 2 and 3 in. This study used Storm 0611 on June 11, 2016 for model calibration, and Tropical Storm Haitang on July 30, 2017 for model validation. In calibrated Model I, the coefficients of efficiency (*CE*) of Stations 1, 2, and 3 were 0.824, 0.989, and 0.951, respectively. In validated Model I, the *CE* values of Stations 1, 2, and 3 were 0.922, 0.995, and 0.981, respectively. In calibrated Model I, the *CE* values of Stations 1, 2, and 3 were 0.847, 0.994, and 0.960, respectively. In validated Model II, the *CE* values of Stations 1, 2, and 3 were 0.916, 0.996 and 0.983, respectively. These *CE* values indicate that the simulated water levels in Model I and Model II were highly accurate. In order to assess the influence of rainfall on the uncertainty of drainage density in the model, the rainfalls of 2-yr, 5-yr, 10-yr, 50-yr, and 100-yr return periods were input into Model I and Model II.

2.3.3 Flooded areas comparison

The differences of simulated flooded areas between Model I, and II were evaluated using three indices, defined as follows. Fig. 3 illustrates the schematic diagram.

$$A(\mathrm{I}-\mathrm{II}) = \mathrm{A(I)} - \mathrm{A(I \cap II)} \quad (2)$$

$$A(\mathrm{II}-\mathrm{I}) = \mathrm{A(II)} - \mathrm{A(I \cap II)} \quad (3)$$

$$P(\mathrm{I \cap II}) = \frac{A(\mathrm{I \cap II})}{\mathrm{A(I \cup II)}} \times 100\% \quad (4)$$

$$P(\mathrm{I}-\mathrm{II}) = \frac{A(\mathrm{I}-\mathrm{II})}{\mathrm{A(I \cup II)}} \times 100\% \quad (5)$$

$$P(\mathrm{II}-\mathrm{I}) = \frac{A(\mathrm{II}-\mathrm{I})}{\mathrm{A(I \cup II)}} \times 100\% \quad (6)$$

Where

$A(\mathrm{I})$ is the simulated flooded area in Model I;

$A(\mathrm{II})$ is the simulated flooded area in Model II;

$A(\mathrm{I \cap II})$ is the simulated flooded area in both Model I and Model II;

$A(\mathrm{I \cup II})$ is the simulated flooded area in Model I or Model II

$A(\mathrm{I}-\mathrm{II})$ is the simulated flooded area in Model I, but not in Model II

$A(\mathrm{II}-\mathrm{I})$ is the simulated flooded area in Model II, but not in Model I;

$P(\mathrm{I \cap II})$ is the percentage of the simulated flooded area in both Model I and Model II;

$P(\mathrm{I}-\mathrm{II})$ is the percentage of the simulated flooded area in Model I, but not in Model II;

$P(\mathrm{II}-\mathrm{I})$ is the percentage of the simulated flooded area in Model II, but not in Model I;

3 Results and discussion

3.1 The result of Experiment I

Table 3, Table 4, and Table 5 depict the results of Experiment I, and Fig. 4 display the simulated flooded areas under 2-yr ~ 100-yr return period rainfall.

Under the 2-year return period rainfall, Drainage 2-yr to Drainage 100-yr had greater flood capacities than the 2-year return period. Therefore, no flooding occurred in Model 2-yr to Model 50-yr, and the Q_A and V_A of all models were 856 cms and 13,795,000 m^3.

Under the 5-year return period rainfall, only Drainage 2-yr had a lower flood capacity than the 5-year return period flood. Since Model 2-yr contained Drainage 2-yr, 25 ha of flooding occurred. The other models did not include Drainage 2-yr, so no flooding occurred. At the same time, the Q_A and V_A in Model 2-yr were 2,111 cms and 38,164,000 m^3, which were smaller than those of other models (2,114 cms and 38,199,000 m^3). Since Model 2-yr contained 25 hectares of flooding, the flood water was retained on the surface, resulting in a decrease in drainage.

Under the 10-year return period rainfall, the 10-year return period flood was greater than the flood capacities of Drainage 2-yr and Drainage 5-yr. In Model 2-yr, 300 ha of flooding occurred in Drainage 2-yr and Drainage 5-yr. Since Model 5-yr contains Drainage 5-yr, 212 ha of flooding occurred. Conversely, Drainage 2-yr and Drainage 5-yr were not set in

other models, so no flooding occurred. Correspondingly, Q_A and V_A of Model 2-yr (2,831 cms and 54,517,000 m^3) were the smallest, followed by the Q_A and V_A of Model 5-yr (2,853 cms and 54,802,000 m^3), and the Q_A and V_A of other models (2,902 cms and 55,188,000 m^3) were the largest.

Because SOBEK is a 1D-2D model, the discharges from Rain-Runoff model are input into the drainages first. If the discharge is less than the flood capacity of the drainage, then flooding does not occur. If the discharge is greater than the flood capacity of the drainage, then flooding occurs. Therefore, the reduction in tributary drainages results in two effects on the simulation results of the 1D-2D model.

Effect 1: Under the same return period rainfall, fewer tributary drainages in a model (lower drainage density) indicates a smaller flooded area.

Effect 2: Under the same return period rainfall, fewer tributary drainages in a model (lower drainage density) indicates an increased peak discharge and total volume of discharge in the drainages.

3.2 Experiment II results

The analysis results are shown in Table 6, Fig 5 and Fig. 6.

Table 6 shows that in all simulated rainfall scenarios, Model II have larger flooding areas than Model I, and A(I) is approximately 83.9 % ~ 96.9 % of A(II). However, P(I ∩ II) is only 49.7 ~ 66.1 %. Thus Models I and II have similar total flooded areas, but significantly different flooded locations, and this difference increases with an increase in rainfall.

The A(II−I) of 2-yr, 5-yr, 10-yr, 50-yr, and 100-yr return period rainfalls were 86.32 ha, 162.16 ha, 329.56 ha, 499.80 ha and 672.32 ha, respectively. However, P(II−I) of 2-yr, 5-yr, 10-yr, 50-yr, and 100-yr return period rainfalls were 31.2 %, 23.7 %, 27.4 %, 18.2 % and 19.8 %, respectively (as shown in Table 6). A(II−I) occurred because farmland drainages were set up in Model II, but not in Model I, so some flooding that occurred in farmland drainages could not be shown in Model I. This caused an underestimate of the flooded area in Model I (Effect 1 had been proved in experiment I). The flood capacity of farmland drainage is almost 2-yr ~ 5-yr return period, and the flood capacity of regional drainage is 10-yr return period. Under 2 return period rainfall, the majority of flooding occurred in farmland drainages, and P(II−I) = 31.2 %. However, the P(II−I) values during the 50-yr or 100-yr return period rainfalls were only 18.2 % and 19.8 %, respectively, because most of the discharges far exceeded the drainage capacities of regional drainages and farmland drainages. In general, A(II–I) increased as the total rainfall rose, and P(I−II) decreased significantly as the total rainfall rose (see Fig 5 and Fig. 6).

The A(I-II) of 2-yr, 5-yr, 10-yr, 50-yr, and 100-yr return period rainfalls were 53.12 ha, 128.68 ha, 162.52 ha, 428.72 ha, and 512.88 ha, respectively. However, P(I−II) of 2-yr, 5-yr, 10-yr, 50-yr, and 100-yr return period rainfalls were 19.2 %, 18.8 %, 13.5 %, 15.6 % and 15.1 %, respectively (see Table 6). A(I−II) occurred because farmland

drainages were set up in Model II, but not in Model I, so some flooding in farmland drainages could not be shown in Model I. Therefore, the peak discharges and volumes of discharges in drainages in Model I were greater than those in Model II (Effect 2 was shown in Experiment I). In Model I, the higher discharges in drainages caused the overflow occurrence at certain downstream reaches, resulting in an overestimate of the flooded area. In general, A(I−II) increased as the total rainfall rose, and P(I-II) declined slightly with increasing total rainfall (see Fig 5 and Fig. 6).

Overall, P(I−II) and P(II−I) decreased with increasing rainfall, and P(I∩II) rose with rising rainfall (see Fig. 6), indicating that the uncertainty of drainage density declined with rising rainfall.

3.3 Discussion

These experimental results indicate that the drainage density in the 1D-2D model had a direct impact on the accuracy of the flood hazard mapping. The analytical results reveal a model with higher drainage density was more similar to the real terrain, and generated more accurate simulation results. However, obtaining detail topographical data of tributary drainages is difficult, expensive and time-consuming. Therefore, in the flooding hazard mapping, we recommend evaluating the drainage density with reference to two factors, the simulated rainfall scenario and the local key areas.

In the model, the determination of drainage density is directly related to the simulated rainfall situation. A higher drainage density should be selected for a lower simulated rainfall level. Conversely, a lower drainage density could be selected given a higher simulated rainfall level. Flood hazard mapping is generally simulated with extreme historical or designed rainfall events, and the models are typically calibrated and verified by the hydrological stations located in rivers (Timbadiya *et al.* 2015; Wilson *et al.* 2007). In this case, the models are normally set up in with only vertical and horizontal sections of the mainstreams. When the extreme flow is greater than the flood discharge capacity of the river, large-scale flooding occurs on both sides of the mainstream, causing flooding in low-lying areas. Conversely, a model for the flood hazard mapping with low return period rainfall, such as 2-yr, 5-yr, and 10-yr should establish tributary drainage, such as regional drainage or farmland drainage, otherwise it might underestimate the simulated flooded area, and skew the location of flooded area.

We recommend raising the drainage density of local key areas in the model, such as important preservation objects and settlements, in the process of flood hazard mapping. Since the flood hazard map is an important basis for the subsequent decision of disaster prevention measures, the accuracy of flooding simulation in some key areas is very important. Therefore, if the drainage density of the entire survey area cannot be increased owing to limitations of funding and data acquisition, then the drainage density can be increased in key regions.

The latest technology can be employed to improve the accuracy of the flood hazard mapping. A large number of tributary drainage data need to be collected, saved and managed in order to improve the accuracy of flooding

simulation. The management platform of the basic data for the model is very important. Performing surveys manually in the field is quite time-consuming and expensive. The digital terrain data can be obtained using drones, and processed through appropriate post-processing technology (Meesuk *et al.* 2015). As well as the calibration and verification of the model, distributed flooding observation data are also required to improve the accuracy of the model, and especially to confirm the accuracy of the flooded area. Smart water level gauges and Internet of Things technology can be efficiently used to obtain a large number of continuous and accurate flooding data (Chang *et al.* 2018). The application of drones for large-scale identification of range of flooding is also a significant direction for future research (Yang *et al.* 2020).

4 Conclusion

Drainage density has a significant impact on the accuracy of the 1D-2D model simulation, but has not been discussed in previous studies. Simplifying the tributary drainages has two main effects under the same rainfall scenario. Under the same return period rainfall, fewer tributary drainages in a model indicates a smaller flooded area (Effect 1), as well as an increased peak discharge and total volume of discharge in the drainages (Effect 2). In the case study of Yanshuixi Drainage, Effect 1 caused an underestimate of the flooded area, and Effect 2 caused an overestimate of the flooded area. The impact of these two effects on the simulation results gradually decreased as the rainfall increased. These characteristics can be utilized to select the appropriate drainage density. If the model is to simulate rainfall with a low return period, then the tributary drainage data cannot be simplified. However, for flood hazard mapping with extreme events, if only mainstreams are set in the model, then the tributary drainages at important locations can be raised to improve the accuracy of the simulation. Manual survey of tributary drainages is costly and time-consuming. For large-scale flood hazard mapping, airborne radar or drones can quickly obtain a large amount of tributary drainage data, making an important future research direction.

References

Adeogun AG, Daramola MO, Pathirana A (2015) Coupled 1D-2D hydrodynamic inundation model for sewer overflow: Influence of modeling parameters Water Science 29:146-155 doi:10.1016/j.wsj.2015.12.001

Apel H, Aronica G, Kreibich H, Thieken A (2009) Flood risk analyses—how detailed do we need to be? Natural Hazards 49:79-98 doi:10.1007/s11069-008-9277-8

Bales J, Wagner C (2009) Sources of uncertainty in flood inundation maps Journal of Flood Risk Management 2:139-147 doi:10.1111/j.1753-318X.2009.01029.x

Chang C-H, Chung M-K, Yang S-Y, Hsu C-T, Wu S-J (2018) A case study for the application of an operational two-dimensional real-time flooding forecasting system and smart water level gauges on roads in Tainan City, Taiwan Water 10:574 doi:10.3390/w10050574

Chiou PT-K, Chen C-R, Chang P-L, Jian G-J Status and outlook of very short range forecasting system in Central Weather Bureau, Taiwan. In: Applications with Weather Satellites II, 2005. International Society for Optics and Photonics, pp 185-197. doi:10.1117/12.601195

de Moel H, Jongman B, Kreibich H, Merz B, Penning-Rowsell E, Ward PJ (2015) Flood risk assessments at different spatial scales Mitigation and Adaptation Strategies for Global Change 20:865-890 doi:10.1007/s11027-015-9654-z

Deltares (2017) SOBEK User Manual.

Dimitriadis P *et al*. (2016) Comparative evaluation of 1D and quasi-2D hydraulic models based on benchmark and real-world applications for uncertainty assessment in flood mapping Journal of Hydrology 534:478-492 doi:10.1016/j.jhydrol.2016.01.020

Doong D-J, Lo W, Vojinovic Z, Lee W-L, Lee S-P (2016) Development of a New Generation of Flood Inundation Maps—A Case Study of the Coastal City of Tainan, Taiwan Water 8:521 doi:10.3390/w8110521

Meesuk V, Vojinovic Z, Mynett AE, Abdullah AF (2015) Urban flood modelling combining top-view LiDAR data with ground-view SfM observations Advances in Water Resources 75:105-117 doi:10.1016/j.advwatres.2014.11.008

Merwade V, Olivera F, Arabi M, Edleman S (2008) Uncertainty in flood inundation mapping: current issues and future directions Journal of Hydrologic Engineering 13:608-620 doi:10.1061/(ASCE)1084-0699(2008)13:7(608)

Noh SJ, Lee J-H, Lee S, Kawaike K, Seo D-J (2018) Hyper-resolution 1D-2D urban flood modelling using LiDAR data and hybrid parallelization Environmental Modelling & Software 103:131-145 doi:10.1016/j.envsoft.2018.02.008

Price R, Vojinovic Z (2008) Urban flood disaster management Urban Water Journal 5:259-276 doi:10.1080/15730620802099721

Teng J, Jakeman AJ, Vaze J, Croke BF, Dutta D, Kim S (2017) Flood inundation modelling: A review of methods, recent advances and uncertainty analysis Environmental modelling & software 90:201-216 doi:10.1016/j.envsoft.2017.01.006

Timbadiya P, Patel P, Porey P (2015) A 1D–2D coupled hydrodynamic model for river flood prediction in a coastal urban floodplain Journal of Hydrologic Engineering 20:05014017 doi:10.1061/(ASCE)HE.1943-5584.0001029

Wang Y, Zhang J, Chang P-L, Langston C, Kaney B, Tang L (2016) Operational C-band dual-polarization radar QPE for the subtropical complex terrain of Taiwan Advances in Meteorology 2016 doi:10.1155/2016/4294271

Werner M (2004) A comparison of flood extent modelling approaches through constraining uncertainties on gauge data Hydrology and Earth System Sciences 8(6):1141-1152

Werner M, Blazkova S, Petr J (2005) Spatially distributed observations in constraining inundation modelling uncertainties Hydrological Processes: An International Journal 19:3081-3096 doi:10.1002/hyp.5833

Wilson M *et al*. (2007) Modeling large-scale inundation of Amazonian seasonally flooded wetlands Geophysical Research Letters 34 doi:10.1029/2007GL030156

Wong JS, Freer JE, Bates PD, Sear DA, Stephens EM (2015) Sensitivity of a hydraulic model to channel erosion uncertainty during extreme flooding Hydrological processes 29:261-279 doi:10.1002/hyp.10148

Wu S-J, Lien H-C, Chang C-H (2010) Modeling risk analysis for forecasting peak discharge during flooding prevention and warning operation Stochastic Environmental Research and Risk Assessment 24:1175-1191 doi:10.1007/s00477-010-0436-6

Wu S-J, Yang J-C, Tung Y-K (2011) Risk analysis for flood-control structure under consideration of uncertainties in design flood Natural hazards 58:117-140 doi:10.1007/s11069-010-9653-z

Wu X, Wang Z, Guo S, Liao W, Zeng Z, Chen X (2017) Scenario-based projections of future urban inundation within a coupled hydrodynamic model framework: A case study in Dongguan City, China Journal of hydrology 547:428-442 doi:10.1016/j.jhydrol.2017.02.020

Yang M-D, Tseng H-H, Hsu Y-C, Tsai HP (2020) Semantic segmentation using deep learning with vegetation indices for rice lodging identification in multi-date UAV visible images Remote Sensing 12:633 doi:10.3390/rs12040633

Yang S-Y, Chan M-H, Chang C-H, Chang L-F (2018a) The Damage Assessment of Flood Risk Transfer Effect on Surrounding Areas Arising from the Land Development in Tainan, Taiwan Water 10:473 doi:10.3390/w10040473

Yang S-Y, Chan M-H, Chang C-H, Hsu C-T (2018b) A case study of flood risk transfer effect caused by land development in flood-prone lowlands Natural Hazards:1-16 doi:10.1007/s11069-017-3130-x

Table 1 Drainages included in various models in Experiment I

Model	Drainage 2-yr	Drainage 5-yr	Drainage 10-yr	Drainage 50-yr	Drainage 100-yr
Model 2-yr	○†	○	○	○	○
Model 5-yr	×‡	○	○	○	○
Model 10-yr	×	×	○	○	○
Model 50-yr	×	×	×	○	○
Model 100-yr	×	×	×	×	○

†: included in the model; ‡: not included in the model

Table 2 Comparison of the drainages and sub-catchments for two models

Model	**Type of Drainage**	**Total area** A **(km^2)**	**Total length of drainage** L **(km)**	**Drainage density** L/A **(km^{-1})**
Model I	Regional Drainage	108.454	75.370	0.695
Model II	Regional Drainage, Farmland Drainage	108.454	125.513	1.157

Table 3 The simulated flooded area under various rainfall scenarios

(unit: ha)

Model	2-yr return period rainfall	5-yr return period rainfall	10-yr return period rainfall	50-yr return period rainfall	100-yr return period rainfall
Model 2-yr	0	25	300	569	844
Model 5-yr	0	0	212	519	791
Model 10-yr	0	0	0	138	411
Model 50-yr	0	0	0	0	278
Model 100-yr	0	0	0	0	0

Table 4 The peak discharge at Point A under various rainfall scenarios

(unit: cms)

Model	2-yr return period rainfall	5-yr return period rainfall	10-yr return period rainfall	50-yr return period rainfall	100-yr return period rainfall
Model 2-yr	856	2,111	2,831	4,463	4,922
Model 5-yr	856	2,114	2,853	4,480	4,940
Model 10-yr	856	2,114	2,902	4,652	5,205
Model 50-yr	856	2,114	2,902	4,708	5,293
Model 100-yr	-*	-	-	-	-

*:There is no Point A in Model 100-yr

Table 5 The simulated total discharge volume at Point A under various rainfall scenarios

(unit: thousand m^3)

Model	2-yr return period rainfall	5-yr return period rainfall	10-yr return period rainfall	50-yr return period rainfall	100-yr return period rainfall
Model 2-yr	13,795	38,164	54,517	89,970	103,325
Model 5-yr	13,795	38,199	54,802	90,475	103,802
Model 10-yr	13,795	38,199	55,188	92,940	107,497
Model 50-yr	13,795	38,199	55,188	93,360	108,405
Model 100-yr	-*	-	-	-	-

*:There is no Point A in Model 100-yr

Table 6 The maximum simulated flooded areas of various return periods in Models I and II

Return Period (year)	A(I) ha	A(II) ha	$\frac{A(\mathrm{I})}{A(\mathrm{II})}$ %	A(I∩II) ha	A(I-II) ha	A(II-I) ha	A(I∪II) ha	P(I∩II) %	P(I-II) %	P(II-I) %
2	190.76	223.96	85.2	137.64	53.12	86.32	277.08	49.7	19.2	31.2
5	522.40	555.88	94.0	393.72	128.68	162.16	684.56	57.5	18.8	23.7
10	872.08	1039.12	83.9	709.56	162.52	329.56	1201.64	59.0	13.5	27.4
50	2241.44	2312.52	96.9	1812.72	428.72	499.80	2741.24	66.1	15.6	18.2
100	2715.68	2875.12	94.5	2202.80	512.88	672.32	3388.00	65.0	15.1	19.8

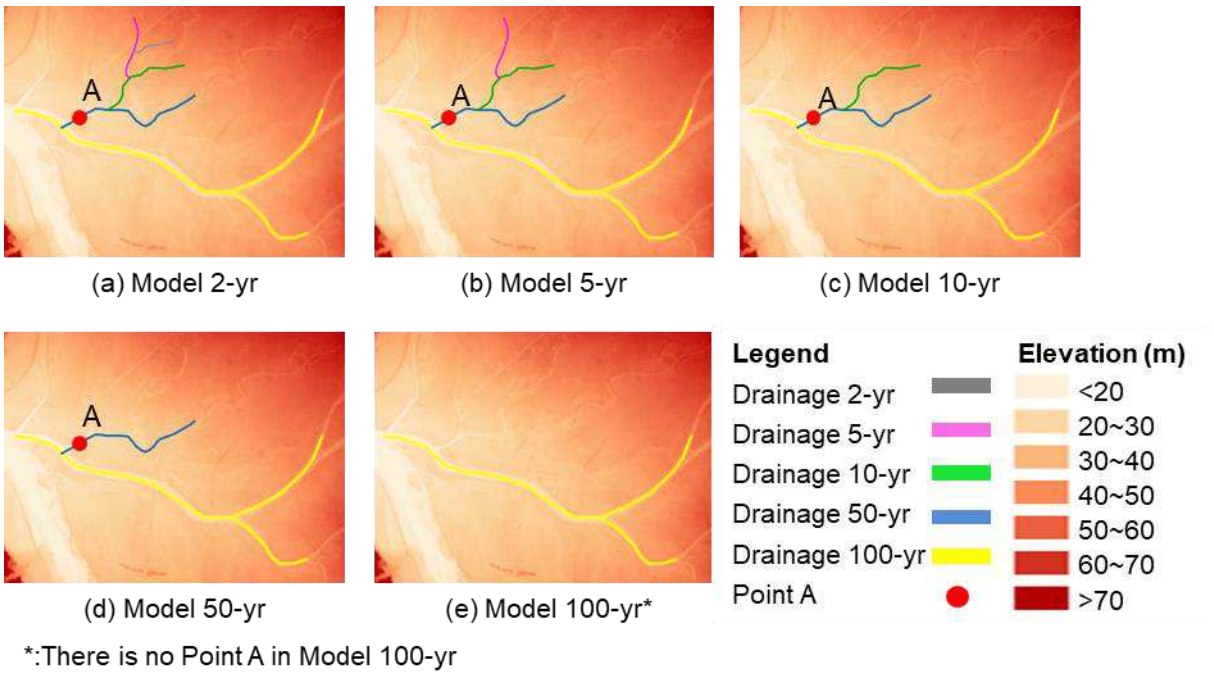

Fig. 1 Drainages included in various models

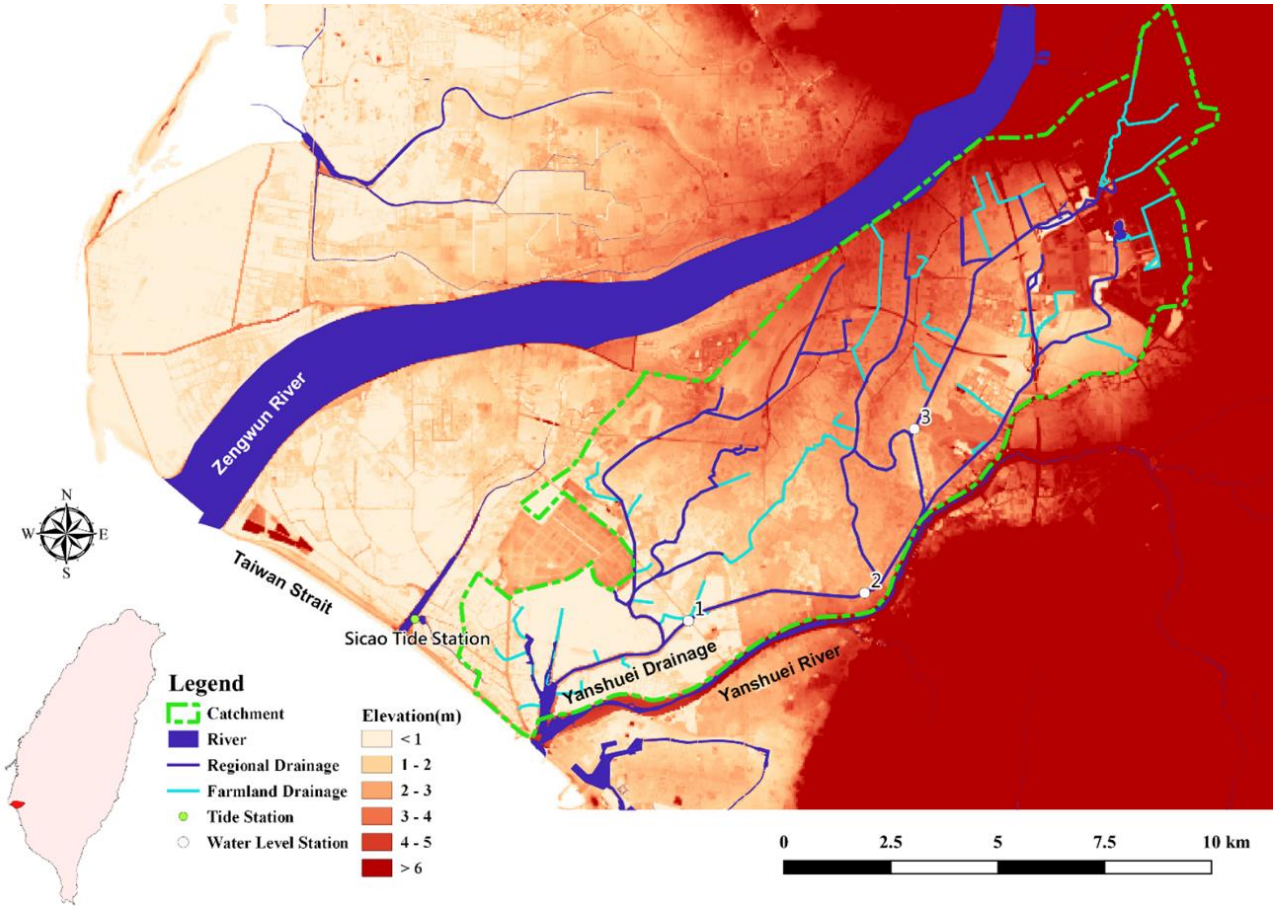

Fig. 2 Location of Yanshuixi Drainage

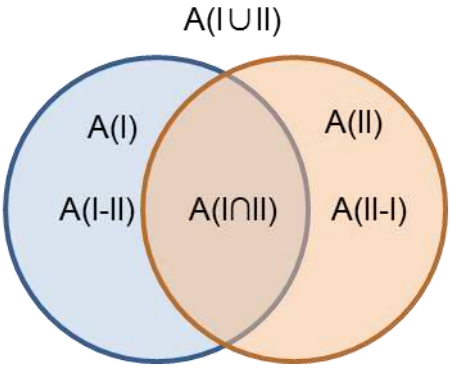

Fig. 3 The schematic diagram comparing flooded areas

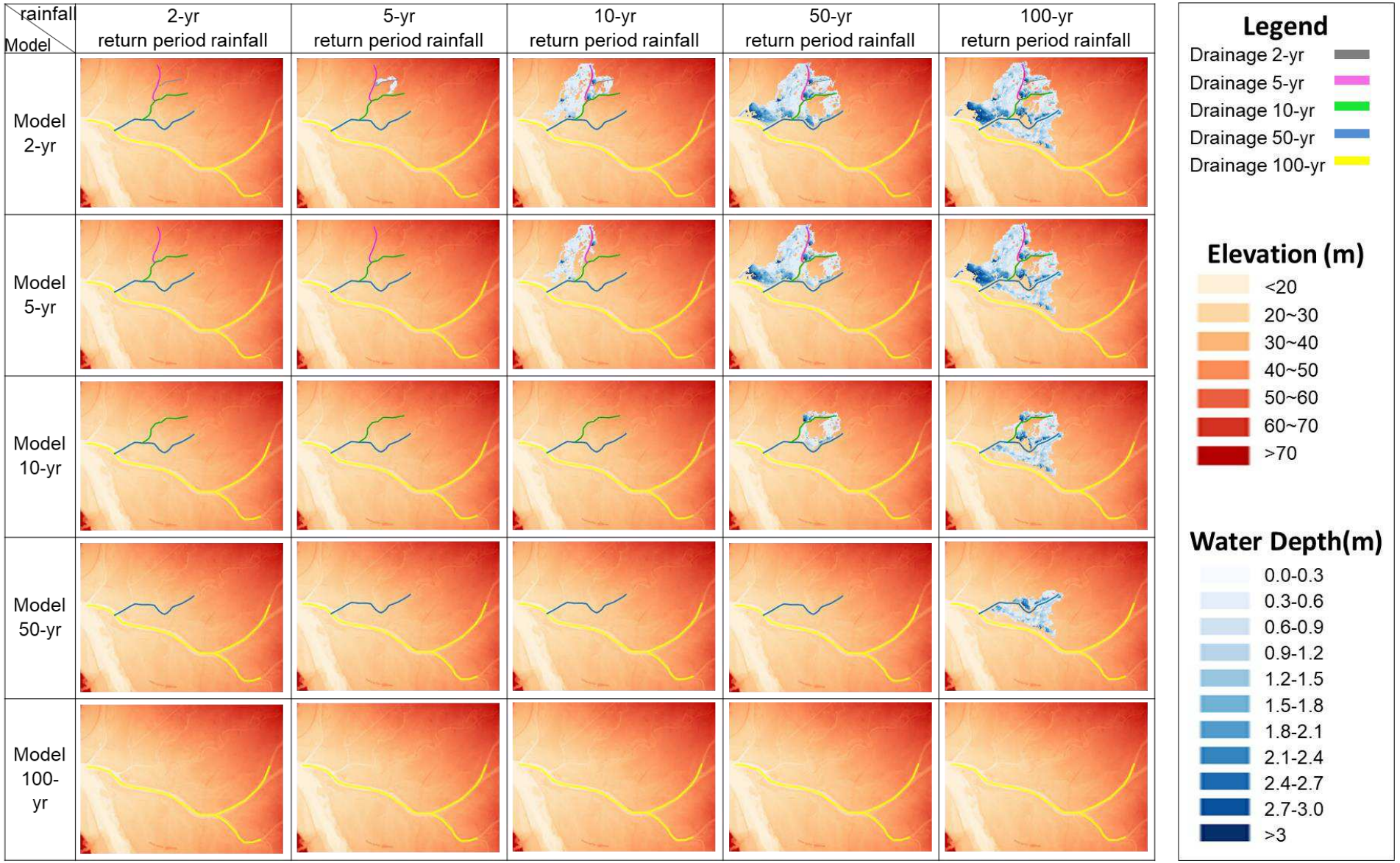

Fig. 4 The simulated flooded areas under 2-yr, 5-yr, 10yr, 50-yr and 100-yr return period rainfall

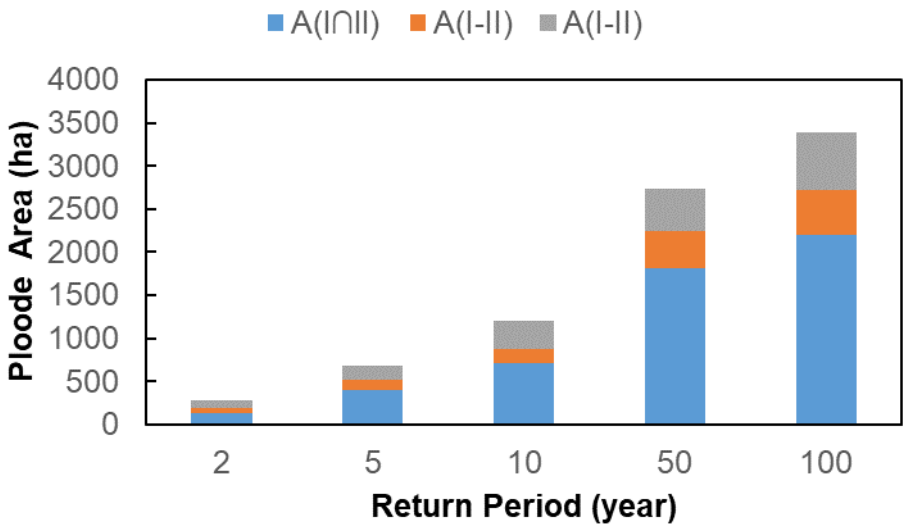

Fig 5 The simulated flooded areas of various return periods

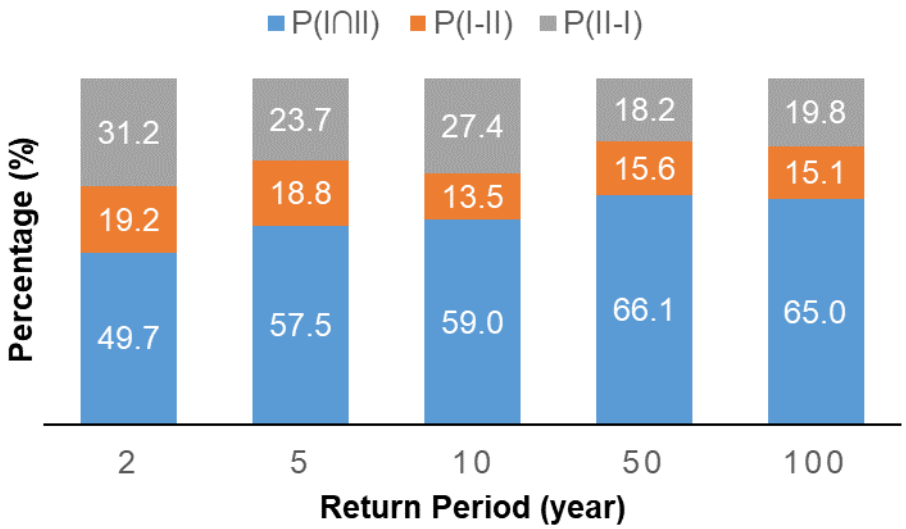

Fig. 6 The percentage of the simulated flooded areas in various return periods